In macrophages, HIV-1 assembles into an intracellular plasma membrane domain containing the tetraspanins CD81, CD9, and CD53

Magdalena Deneka,[1,2] Annegret Pelchen-Matthews,[1,2] Rahel Byland,[1,2] Ezequiel Ruiz-Mateos,[1,2] and Mark Marsh[1,2]

[1]Cell Biology Unit, Medical Research Council Laboratory for Molecular Cell Biology, and [2]Department of Biochemistry and Molecular Biology, University College London, London WC1E 6BT, England, UK

In macrophages, HIV-1 has been shown to bud into intracellular structures that contain the late endosome marker CD63. We show that these organelles are not endosomes, but an internally sequestered plasma membrane domain. Using immunofluorescence microscopy and immunoelectron microscopy, we find that HIV-1 buds into a compartment that contains the tetraspanins CD81, CD9, and CD53. On uninfected macrophages, these proteins are seen at the cell surface and in intracellular vacuole-like structures with a complex content of vesicles and interconnected membranes that lack endosome markers, including CD63. Significantly, these structures are accessible to small tracers (horseradish peroxidase or ruthenium red) applied to cells at 4°C, indicating that they are connected to the cell surface. HIV assembles on, and accumulates within, these intracellular compartments. Furthermore, CD63 is recruited to the virus-containing structures and incorporated into virions. These results indicate that, in macrophages, HIV-1 exploits a previously undescribed intracellular plasma membrane domain to assemble infectious particles.

Introduction

Assembly of the human immunodeficiency virus type 1 (HIV) is a highly regulated process that requires the spatially and temporally coordinated recruitment of viral components, as well as key cellular proteins, to an appropriate membrane system. The site of HIV budding has been reported to vary for different host cells; in T cells and several nonhematopoietic cell lines, the majority of virus particles assemble at the cell surface, but in macrophages these events occur almost entirely on intracellular membranes (Gendelman et al., 1988; Orenstein et al., 1988; Raposo et al., 2002; Pelchen-Matthews et al., 2003). Immunolabeling indicates that the intracellular sites of assembly in these cells are enriched in major histocompatibility complex class II (MHC-II) molecules, suggesting that they are MHC-II compartments (MIICs) where MHC-II molecules acquire their peptide cargo (Raposo et al., 2002). In support of this view, the intracellular virus-containing compartments (VCCs) also label for some markers of late endosomes, such as the tetraspanin CD63 (Raposo et al., 2002; Pelchen-Matthews et al., 2003; Kramer et al., 2005). Several studies with T cells, or cell lines such as HeLa, COS, or HEK293, have also demonstrated a limited and/or transient association of assembling HIV, or of Gag-based virus-like particles, with CD63-containing late endosomes (Nydegger et al., 2003; Sherer et al., 2003; Grigorov et al., 2006; Perlman and Resh, 2006), suggesting an association between HIV assembly and late endosomes in most cells (Resh, 2005). Nonetheless, many studies of T cells and nonhematopoietic cells producing HIV clearly show virus particles budding from the cell surface. This view is supported by several recent studies indicating that HIV Gag is targeted directly to the plasma membrane (Harila et al., 2006; Neil et al., 2006), probably through a specific interaction of the matrix component of Gag with the plasma membrane lipid phosphatidylinositol 4,5-bis-phosphate (PI[4,5]P_2; Ono et al., 2004; Saad et al., 2006), and that HIV particles only reach endosomes as a result of endocytosis of virions formed at the cell surface. It has been suggested that this may also be the case for the intracellular accumulations of HIV seen in macrophages (Jouvenet et al., 2006).

M. Deneka and A. Pelchen-Matthews contributed equally to this paper.

Correspondence to Mark Marsh: m.marsh@ucl.ac.uk

Abbreviations used in this paper: DC, dendritic cell; HIV, human immunodeficiency virus type 1; MDM, monocyte-derived macrophages; MHC-II, major histocompatibility complex class II; MIIC, MHC-II compartment; MVB, multivesicular body; PAG, protein A-gold; PBMC, peripheral blood mononuclear cell; PI(4,5)P_2, phosphatidylinositol 4,5-bis-phosphate; RR, ruthenium red; VCC, intracellular virus-containing compartment.

The online version of this article contains supplemental material.

The Journal of Cell Biology, Vol. 177, No. 2, April 23, 2007 329–341
http://www.jcb.org/cgi/doi/10.1083/jcb.200609050

Much of the evidence for HIV association with endosomes is based on immunolabeling for CD63. CD63 is a well-established marker for late endosomes, which are often multivesicular bodies (MVBs), where it is particularly enriched on the intralumenal vesicles (Escola et al., 1998; Kobayashi et al., 2000). Several other members of the tetraspanin superfamily have also been reported to be associated with MVB. In particular, CD53, CD81, and CD82 have been found to localize to MVB in B cells and are enriched on exosomes, which are the secreted MVB intralumenal vesicles derived from these cells (Escola et al., 1998; Fritzsching et al., 2002). Similarly, CD9 has been found on exosomes from dendritic cells (DCs; Thery et al., 1999). Like CD63, CD81 can be incorporated into the envelope of infectious HIV produced by human monocyte–derived macrophages (MDMs; Nguyen et al., 2003; Pelchen-Matthews et al., 2003). Indeed, tetraspanin microdomains containing CD81 and CD63 have been proposed as sites of HIV assembly and release (Booth et al., 2006; Nydegger et al., 2006).

To further characterize the HIV assembly compartment in human primary MDMs, particularly in regard to its tetraspanin content, we have studied the distribution of CD81 and the related tetraspanins, CD9 and CD53. We show that in uninfected MDMs, these molecules are located at the plasma membrane and in intracellular structures with a complex array of internal CD81/CD9-labeled membrane vesicles and networks. These structures can be reached by antibodies internalized from the cell surface, but are distinct from early endosomes and from the late endosomes and lysosomes identified by CD63 and LAMP-1. On HIV-infected MDMs, virus particles bud into this intracellular CD81/CD9/CD53-containing compartment. Significantly, the VCCs are linked to the cell surface by narrow membrane channels. Notably, HIV infection recruits CD63 to the CD81/CD9/CD53-positive VCCs. Thus, it appears that the HIV assembly compartment in macrophages is not a conventional late endosome, but an internally sequestered plasma membrane domain to which the late endosome marker CD63 is recruited during virus assembly in HIV-infected cells.

Results

In macrophages, HIV assembles in a compartment containing CD63, CD81, and CD9

Previous analyses of HIV-infected MDMs indicated that most virus particles assemble on intracellular structures that contain markers for late endosomes, particularly CD63 (Raposo et al., 2002; Pelchen-Matthews et al., 2003). Indeed, CD63 and another tetraspanin, CD81, are incorporated into the envelope of MDM-derived infectious HIV particles (Nguyen et al., 2003; Pelchen-Matthews et al., 2003). To examine in more detail the distribution of viral antigens compared with these cellular tetraspanins in infected macrophages, we immunolabeled whole cells or semithin (0.5 μm thick) cryosections for virus particles and for CD63, CD81, or the related tetraspanin, CD9 (Fig. 1 and Fig. S1, available at http://www.jcb.org/cgi/content/full/jcb.200609050/DC1). Immunofluorescence revealed the usual distribution for CD63 in MDMs (Fig. 1, top row; Astarie-Dequeker et al., 2002), with the tubulovesicular pattern being reminiscent of the tubular lysosomes described in mouse macrophages (Swanson et al., 1987; Heuser, 1989; Robinson et al., 1996). In contrast, the viral antigens,

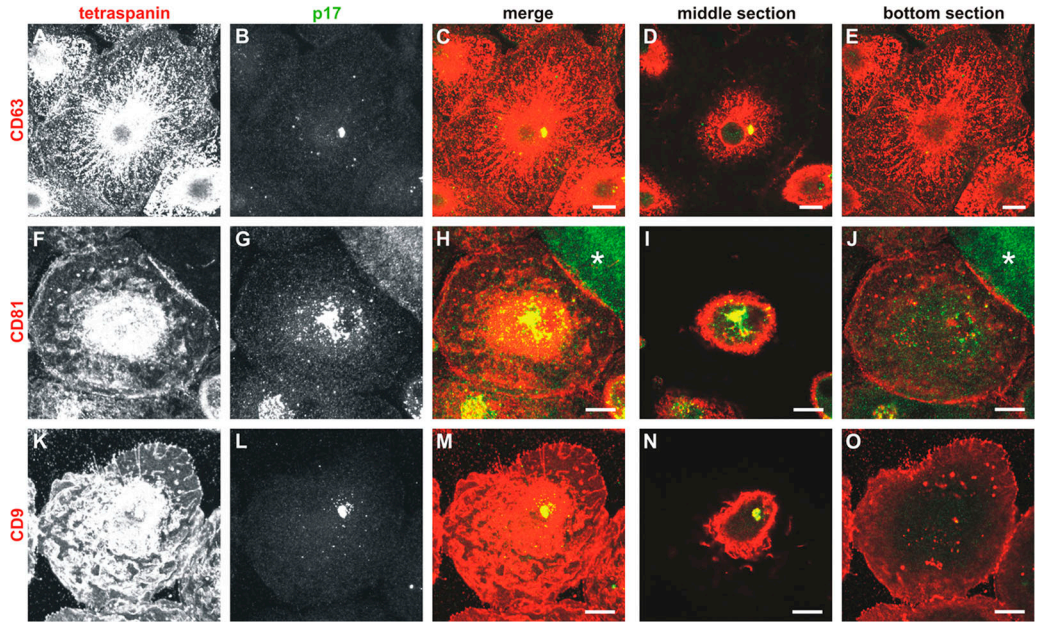

Figure 1. **Colocalization of HIV with CD63, CD81, or CD9.** Primary human MDMs infected with HIV for 10 d were fixed and stained with mouse mAbs against CD63 (A–E), CD81 (F–J), or CD9 (K–O) and rabbit anti-HIV p17, followed by secondary anti–mouse Alexa Fluor 594 and anti–rabbit Alexa Fluor 488 antibodies, and analyzed by confocal microscopy. A–C, F–H, and K–M show projections of 11, 20, and 21 confocal sections, respectively, whereas the images in the two right-hand columns are 0.5-μm-thick confocal sections from the center (D, I, and N) or near the bottom of the cells (E, J, and O). CD63 was found in an extensive network of tubules and vesicles, and also stained the focus of viral p17 (A–D). CD81 and CD9 strongly decorated the cell surface (F and K), but also intracellular puncta near the bottom of the cells (J and O). On medial sections (I and N), the CD81 and CD9 labeling overlapped with the HIV-containing compartment. The asterisk in H marks HIV staining in a syncytium nearby. Bars, 10 μm.

identified with rabbit antibodies against the viral matrix protein p17 (Fig. 1 B and S1 B) or p24 (not depicted) had a much more restricted distribution and appeared to be associated with a subset of the CD63-containing organelles. The distributions of CD81 and CD9 differed from that of CD63; mAbs to both CD81 and CD9 strongly labeled the plasma membrane of infected MDMs (Fig. 1, F and K) and, in addition, stained several punctate intracellular structures (Fig. 1, J and O). In particular, the VCCs were strongly labeled for CD81 and CD9 (Fig. 1, I and N, and Fig. S1). This suggests that CD81 and CD9 more closely identify the HIV-containing subpopulation of CD63-labeled organelles. However, the distribution of CD81 and CD9 has not been looked at systematically in uninfected MDMs.

CD63, CD9, CD53, and CD81 in uninfected MDMs

Although many tetraspanins are prominently expressed at the plasma membrane, several have been found to be associated with intracellular compartments, including late endosomes. In particular, CD9, CD53, CD81, and CD82 have been localized to the intralumenal vesicles of MVBs or found on exosomes from B cell or DC lines (Escola et al., 1998; Thery et al., 1999). We analyzed the distribution of these markers in uninfected MDMs by immunofluorescence microscopy. As in the HIV-infected MDMs, CD63 was found in a tubuloreticular network extending throughout the cells (Fig. 2 A). CD9, CD53, and CD81 showed a distinct distribution. On single confocal sections, CD9 and CD53, for example, were seen at the plasma membrane and also in discrete intracellular puncta (Fig. 2, B and C). These puncta measured up to 2–3 μm in diameter, and were larger than the CD63-containing structures, which did not exceed 0.5 μm diam. Typically, cells contained 20–30 of the larger CD9/CD53/CD81-labeled structures, often close to or extending to ~2.5 μm from the base of the cell.

Fig. 2 D shows by double labeling immunofluorescence that the majority of CD63 in uninfected MDMs was present on LAMP-1–positive tubules and vesicles. As suggested by the distributions described in the previous paragraph, there was no detectable overlap of the CD63-labeled network with the punctate staining for CD81 (Fig. 2 E). Instead, CD9, CD81, and CD53 colocalized extensively with each other, both at the cell surface and in the intracellular puncta, shown here by costaining of CD9 with CD53 or CD81 (Fig. 2, F and G, respectively). To rule out the possibility that these structures represent a subset of early endosomes, we costained the cells with an early endosome marker, EEA1. CD63 and CD9 showed only limited overlap with EEA1 (Fig. 2, H and I). The degree of colabeling was quantified using Volocity. This confirmed a high degree of colocalization between CD63 and LAMP-1 (94%), or between CD9 and CD81 or CD53 (84 and 85%, respectively). In contrast, there was minimal overlap between CD63 and CD81 or EEA1 (26 and 15%, respectively), and between CD9 and EEA1 (~20%), indicating the presence of discrete structures containing either CD63 or the other tetraspanins, which are all largely distinct from early endosomes.

The CD81/CD9/CD53 compartment is accessible to antibodies fed at 37°C

To investigate whether the CD81/CD9/CD53-containing compartment in MDMs is related to the endosome system and whether it can be accessed from the plasma membrane, we

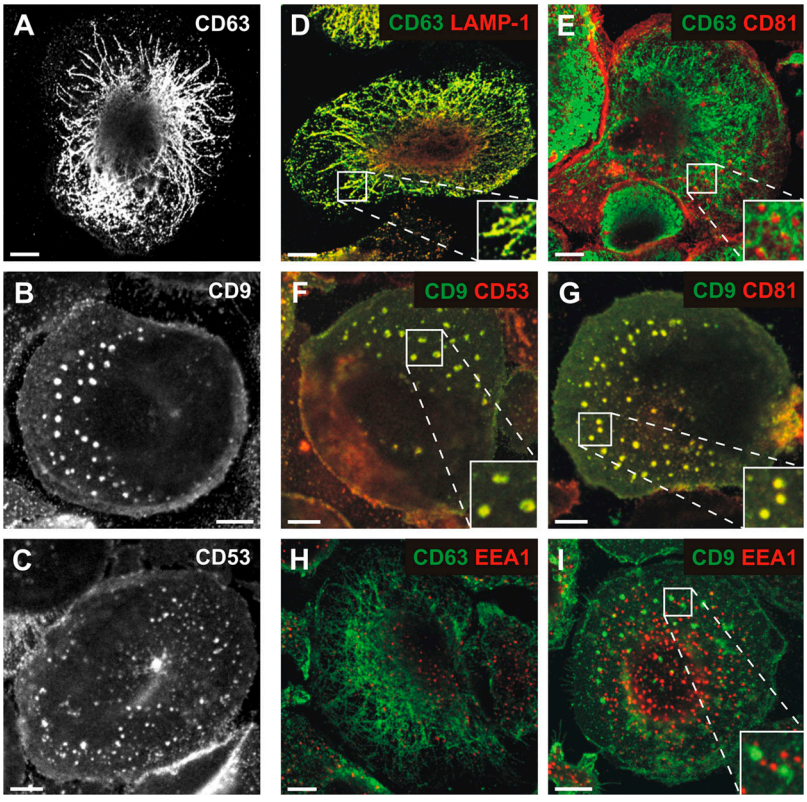

Figure 2. **Distribution of tetraspanins in uninfected MDMs.** MDMs were grown for 16 d, fixed, and stained with mAbs against CD63 (A), CD9 (B), or CD53 (C) and anti–mouse Alexa Fluor 488. CD63 labeled a network of tubular structures, whereas CD9 and CD53 localized to the cell surface and discrete intracellular puncta. To identify these puncta, cells were double stained with mouse IgG1 mAbs to LAMP-1, CD81, CD53, or EEA1, detected with anti–mouse IgG1-Alexa Fluor 594 (red), and IgG2b mAbs to CD63 or CD9, detected with anti–mouse IgG2b-Alexa Fluor 488 (green). CD63 staining overlapped with LAMP-1 (D), but there was almost no colocalization of CD63 with CD81 (E). CD9 labeling showed nearly complete overlap with CD53 (F) or CD81 (G). Neither CD63 (H) nor CD9 (I) colocalized with EEA1. The images show single confocal sections ~1 μm from the bottom of the cell. For D–G and I, the insets show enlargements. Bars, 10 μm.

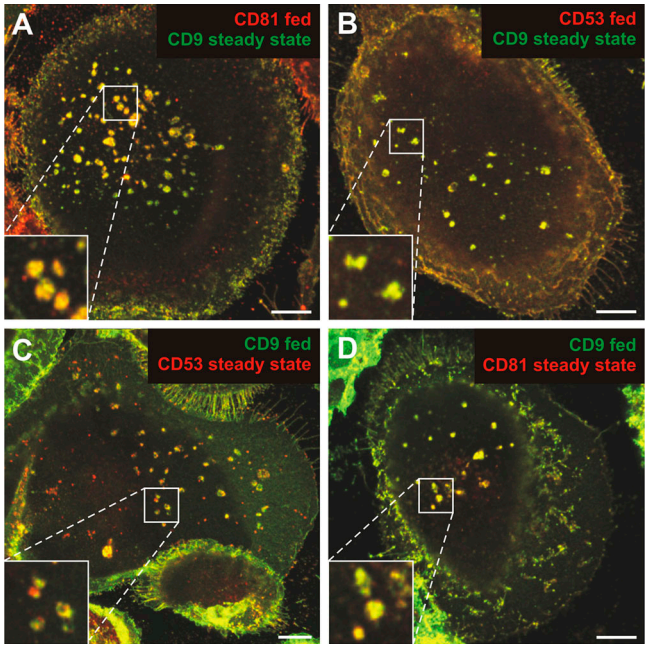

Figure 3. **Uptake of antibodies directed against tetraspanins.** MDMs cultured for 13 d were incubated for 3 h at 37°C in medium containing mAbs against CD81, CD53, or CD9 (fed). Cells were then fixed, permeabilized, and stained with antibodies against a different tetraspanin (steady-state). Antibodies were detected with isotype-specific secondary antibodies (red, anti–mouse IgG1-Alexa Fluor 594, for CD81 and CD53; green, anti–mouse IgG2b-Alexa Fluor 488, for CD9). CD9 colocalized with internalized anti-CD81 (A) or anti-CD53 (B). Similarly, internalized anti-CD9 was found in intracellular structures positive for CD53 (C) or CD81 (D). The images are from single confocal sections ~1 μm from the bottom of the cell, and selected areas are shown enlarged in the insets. Bars, 10 μm.

performed antibody-feeding experiments. Uninfected MDMs were incubated for 3 h at 37°C with mAbs to CD81, CD9, or CD53, and then fixed, permeabilized, and processed for immunofluorescence labeling. The antibodies strongly stained the cell surface (Fig. S2, A and D, available at http://www.jcb.org/cgi/content/full/jcb.200609050/DC1). In addition, some of the antibodies were taken up into intracellular vesicles resembling the aforementioned puncta (Fig. S2), whereas an irrelevant control antibody did not enter the cells under these conditions (not depicted). To test whether the internalized antibodies could access the CD81/CD9/CD53-containing compartment, antibody-feeding experiments were combined with steady-state staining for different tetraspanins. Fig. 3 shows that anti-CD81 or -CD53 mAbs could reach the CD9-positive compartment (Fig. 3, A and B), and internalized anti-CD9 mAbs colocalized with CD53 and CD81 (Fig. 3, C and D). Uptake of the antitetraspanin mAbs was temperature dependent, and labeling was restricted to the cell surface after incubation at 4°C (Fig. S2, B and E). This indicates that the CD81/CD9/CD53-containing compartment can be reached by antibodies fed from the cell surface at 37°C, although the mechanism of uptake remains unknown.

Ultrastructure of the CD81/CD9/CD53 compartment

To analyze the morphology of the MDM CD81/CD9/CD53-containing compartment in more detail, ultrathin cryosections

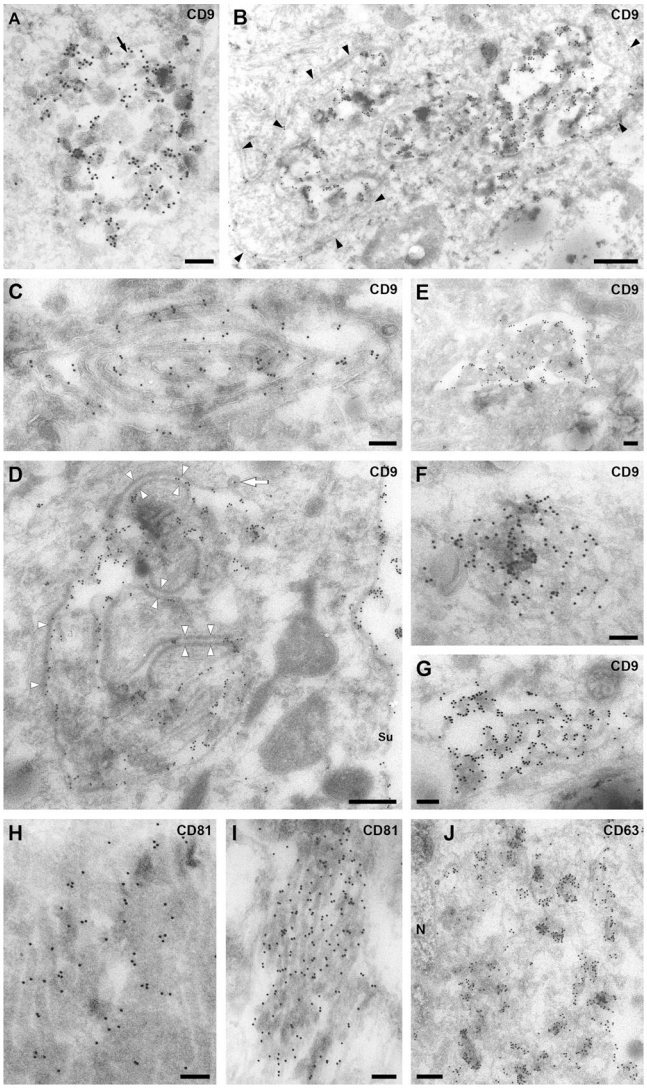

Figure 4. **EM analysis of the CD81- and CD9-containing compartment in uninfected MDMs.** Ultrathin cryosections from uninfected MDMs (14 d after isolation in A, B, E, and G–I; 26 d after isolation in C, D, F, and J) were stained with mouse mAbs against CD9 (A–G), CD81 (H and I) or CD63 (J), followed by a rabbit anti–mouse IgG bridging antibody and PAG (A–I, 15 nm; J, 10 nm). The black arrow in A marks some small (50 nm diam) vesicles reminiscent of the intralumenal vesicles of MVBs. Black arrowheads in B identify apposed membrane sheets, and the white arrowheads in D show a thick coating on some of these apposed membrane sheets. The white arrow marks a coated pit. Su, cell surface; N, nucleus. Bars: (A, C, and E–J) 200 nm; (B and D) 500 nm.

were labeled with anti-CD9 or -CD81 mAbs and protein A-gold (PAG) and examined by EM. On sections labeled for CD9, abundant gold particles were found over cell surface microvilli and membrane ruffles. In addition, we occasionally observed labeling over three types of intracellular structures. The first type is large vacuole-like structures (1–1.5 μm diam) containing various internal membranes, ranging from 50 nm diam vesicles resembling the intralumenal vesicles of MVBs to larger membranes (Fig. 4 A and B). The second type is composed of extended membrane swirls, usually consisting of two closely apposed membranes separated by a narrow gap (Fig. 4 C and D). These are likely to be profiles of larger membrane sheets in

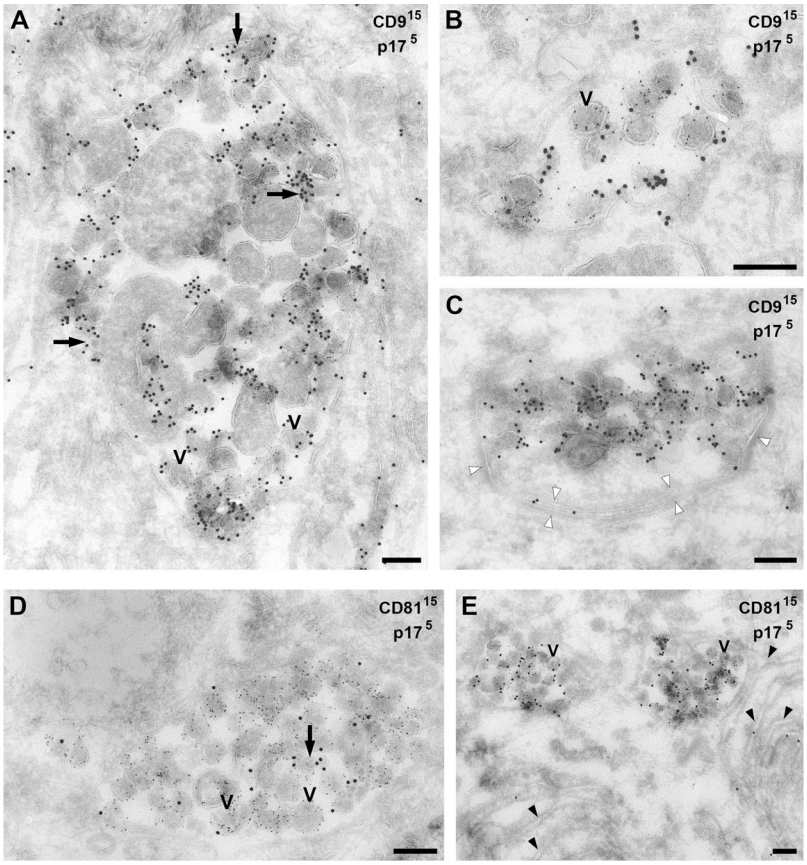

Figure 5. **CD9 and CD81 in VCCs in MDMs.** Ultrathin cryosections from MDMs infected with HIV for 7 d were double labeled with mouse mAbs against CD9 (A–C) or CD81 (D and E) and 15 nm PAG, followed by rabbit anti-p17 and 5 nm PAG. HIV virions are identified by their characteristic size (120–140 nm diam) and morphology and by labeling with 5 nm PAG (some virions are marked V in A–E). CD9 and CD81 are found in the VCCs, occasionally even in the viral envelopes, as well as over internal membranes of various sizes and including small (50 nm diam) vesicles (A and D, black arrows). Note the thick protein coat on the apposed membrane sheets in C (white arrowheads) and the extended areas of closely apposed membrane sheets in E (black arrowheads). Bars, 200 nm.

the sections. Occasionally, such membranes were lined with an extended dense coat (Fig. 4 D), and some MVB-like structures had extensions of the apposed parallel membrane sheets (Fig. 4 B). The third type appeared like arrays of highly interconnected membranes (Fig. 4, E–G and I). These structures were not enclosed in a continuous limiting membrane, allowing extensions of the cytoplasm into the membrane meshwork and giving it a spongelike appearance. The compartments identified by the anti-CD9 or -CD81 antibodies differed from the structures labeled for CD63. In keeping with the many small vesicles and tubulovesicular structures seen by immunofluorescence, anti-CD63 antibodies labeled various small membrane vesicles and tubules, often close to the nucleus (Fig. 4 J). This, again, indicates that CD63 and the tetraspanins CD81, CD9, and CD53 are located in distinct structures in uninfected MDMs.

HIV assembles in the CD81/CD9/CD53 compartment

Immunofluorescence staining of HIV-infected MDMs demonstrated that the virus, which was detected with anti-p17, was localized to VCCs that costained with CD81, CD9 (Fig. 1 and Fig. S1), and CD53 (not depicted), indicating that HIV assembles in the CD81/CD9/CD53 compartment. The VCCs appeared larger and more irregular than the CD81/CD9/CD53-containing puncta seen in uninfected MDMs, and were usually located higher in the cell (compare Fig. 1, D, I and N with E, J, and O), suggesting that HIV infection may expand the CD81/CD9/CD53-containing structures or cause them to coalesce. In addition to staining of the VCCs, some tetraspanin labeling was also observed in virus-negative intracellular puncta in the cells and at the plasma membrane, indicating that viral components are directed to a subset of the CD81/CD9/CD53-containing membranes. Little, if any, labeling for p17 was seen at the cell surface.

EM immunolabeling of ultrathin cryosections of HIV-infected MDMs revealed VCCs that resembled the intracellular CD81- or CD9-labeled structures seen in uninfected cells. The sections in Fig. 5 were double-labeled with 5 nm PAG marking p17 and 15 nm PAG identifying CD9 or CD81. Virus particles labeled for p17 could be seen in a variety of structures ranging from 0.5 μm to several micrometers in diameter (Fig. 5, A and B), some of which also contained internal vesicles and larger membranes that labeled strongly for CD9 (Fig. 5 A) and resembled the multivesicular structures shown in Fig. 4 (A and B). The VCCs in Fig. 5 C also has patches of flat coat on its limiting membrane (compare with Pelchen-Matthews et al., 2003) and a long, curved double-membrane sheet linking its two poles. Double labeling for virus and CD81 revealed similar structures. The VCC in Fig. 5 D contains some CD81-labeled small vesicles similar to MVB intralumenal vesicles. Two small VCCs in Fig. 5 E appear to be connected to extended CD81-labeled parallel membrane tracks (the extent of these membranes is shown at lower magnification in Fig. S3 A, available at http://www.jcb.org/cgi/content/full/jcb.200609050/DC1).

The virus assembly compartment in Epon-embedded MDMs

Transmission EM of plastic-embedded, HIV-infected MDMs, where the ultrastructure of virus particles is much clearer, also indicated that HIV accumulated in intracellular structures that morphologically resembled the CD9- or CD81-labeled organelles observed on cryosections. Virions were found in VCCs in the juxtanuclear area (Fig. 6 A). Often, several such VCCs were located in close proximity, separated by thin membrane bridges, or with fingerlike membrane projections protruding into their interior (Fig. 6 B). Occasionally, coated pits could be seen on the limiting membranes. Other VCCs were associated with extended swirls of closely apposed membrane sheets (Fig. 6, C and D). Fig. 6 E shows part of a large VCC in the vicinity of an unusual structure consisting of highly interconnected membranes. Although this had an overall rounded appearance, it lacked a continuous limiting membrane, so that tracks of cytoplasm permeated deep into the membrane meshwork. This structure resembles the spongelike structures labeled for CD9 or CD81 (compare Fig. 4, E–G and I, respectively). In Fig. 6 E, a spongelike structure was located near a VCC, and many other VCCs were found close to, or appeared to arise from, such structures. For example, Fig. 6 F shows an extended area of interconnected membrane meshwork with peripheral pockets of virus particles; indeed, one virion can be seen in the center of the spongelike region (Fig. 6 F, V). Smaller interconnected membranes, which might be residues of spongelike elements, were also apparent in Fig. 6 G (asterisks). The presence of budding figures and immature virus particles within these structures, and association with the interconnected sponge membranes (Fig. 6 G, arrowheads), indicates that HIV particles are assembled on these membranes. Overall, spongelike structures of various sizes were found associated with ∼30% of the VCCs. Although these structures were relatively rare in the MDMs, their frequent association with HIV assembly sites indicates that they are involved in virus budding, perhaps providing a source of membranes to form the viral envelopes.

Analysis of serial sections of HIV-infected macrophages by EM (Fig. 7) further demonstrated the complexity of the virus assembly compartments. Although the end sections show relatively simple VCCs (Fig. 7, K or L), the central sections (Fig. 7, D–I) reveal interconnected chambers and a large spongelike region surrounded by assembled viruses. Budding profiles and

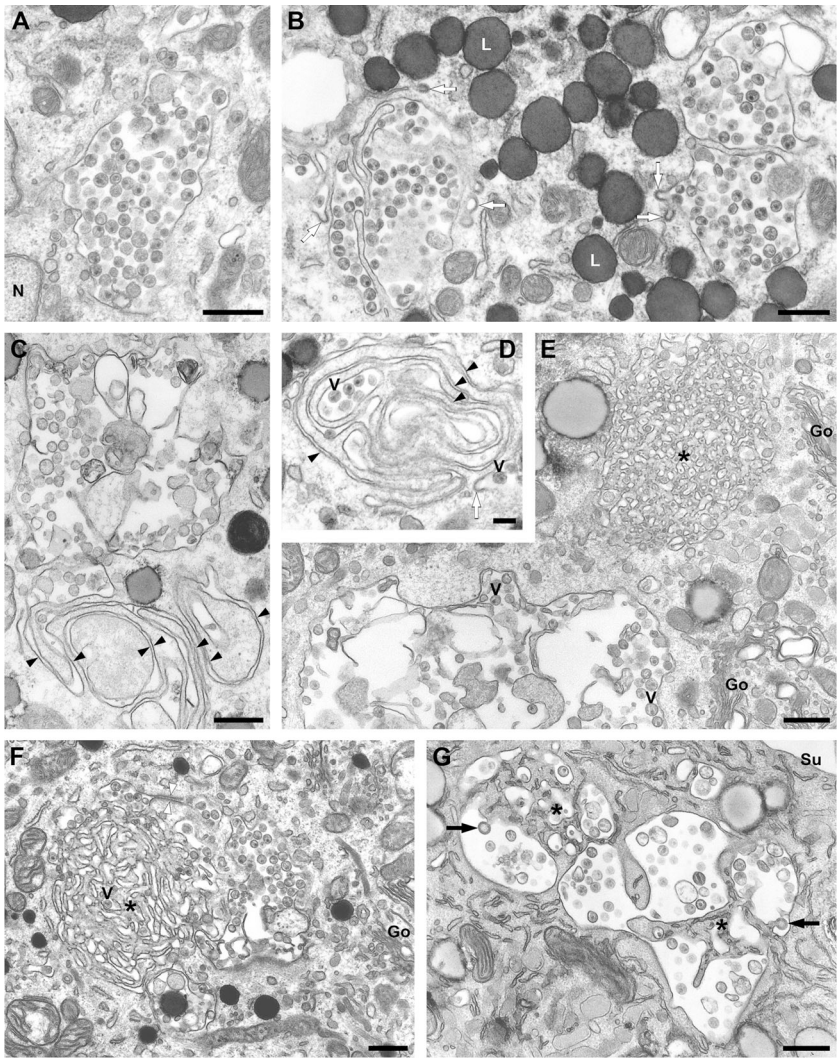

Figure 6. **Morphology of VCCs in HIV-infected MDMs.** MDMs infected with HIV for 14 d (or 13 d for the cell shown in G) were fixed and embedded in Epon for transmission EM. (A and B) Virus particles, identified by their characteristic morphology, were seen in VCCs in the juxtanuclear region. Note the coated pits associated with the VCCs (white arrows in B). N, nucleus; L, lipid droplets. (C and D) VCCs associated with extended swirls of closely apposed membrane sheets (black arrowheads; V marks some of the virions in D). (E) A spongelike meshwork of interconnected membranes (asterisk) near a large, swollen VCC. V, virus particle; Go, Golgi complex. (F and G) Spongelike interconnected membranes (F) or remnants of such structures (G, asterisks) were frequently seen associated with VCCs. (V marks a virion deep in a membrane-sponge in F, white arrowheads show coated apposed membranes, black arrows indicate budding virus particles in G). Su, cell surface. Bars: (A–C and E–G) 500 nm; (D), 200 nm.

immature virus particles are apparent on several of the panels (Fig. 7, A, B, and G–K), indicating that HIV assembly occurs directly into this compartment. Some buds can even be seen to arise from the spongelike structure in the core of the VCCs (Fig. 7 G). Significantly, although budding profiles and virus particles could be seen in intracellular VCCs, no such structures were found at the cell surface (Fig. S4 A, available at http://www.jcb.org/cgi/content/full/jcb.200609050/DC1). The serial section images in Fig. S4 show that even apparently dispersed VCCs are connected in some sections and associated with condensed spongelike structures. Some VCCs were connected to membrane tracks or parallel membrane sheets (Fig. 6, C and D; and Fig. S3), suggesting that they may be linked by elongated tubular extensions or via the closely apposed membrane sheets, and raised the possibility that some apparently intracellular VCCs may be connected to the cell surface.

The VCCs are connected to the cell surface

To test whether the VCCs are accessible from the cell surface, HIV-infected or uninfected MDMs fed for 3 h with anti-CD81 mAb, were cooled on ice and incubated for 1 h at 4°C in medium containing 10 mg/ml HRP. Subsequently, the cells were fixed and prepared for cryosectioning. Immunofluorescence staining of semithin cryosections for HIV p17, CD81, and HRP indicated that the HRP had reached the CD81-labeled VCC, even though this structure appeared to be located deep within the cell (Fig. 8, A–E). Similarly, HRP could access many of the puncta into which CD81 antibodies were internalized on uninfected cells (Fig. 8, F–J). Surface connections were also apparent on HIV-infected macrophages fixed in the presence of the electron-dense, cell-impermeant dye ruthenium red (RR). HIV particles located in apparently intracellular VCCs and clearly identified by their characteristic morphology were coated with a layer of RR (Fig. 8 K). The dye appeared to gain access to the virus particles through the narrow gaps between closely apposed membrane sheets, which could be traced from the cell surface to the deep VCCs (Fig. 8 L). Indeed, most of the VCCs in this image appear to be connected by narrow membrane tracks. The surface connections were particularly clear on serial sections. The images in Fig. 8 (N–Q) show a narrow RR-stained channel linking three interconnected VCCs to the cell surface. Although the VCCs were accessible to a tracer from the extracellular medium, the connecting membrane tracks were always very narrow. The space between the membrane sheets appears to be ~15–20 nm on Epon sections, or 25–30 nm on cryosections, which is far too narrow for virions (~140 nm diam) to pass through.

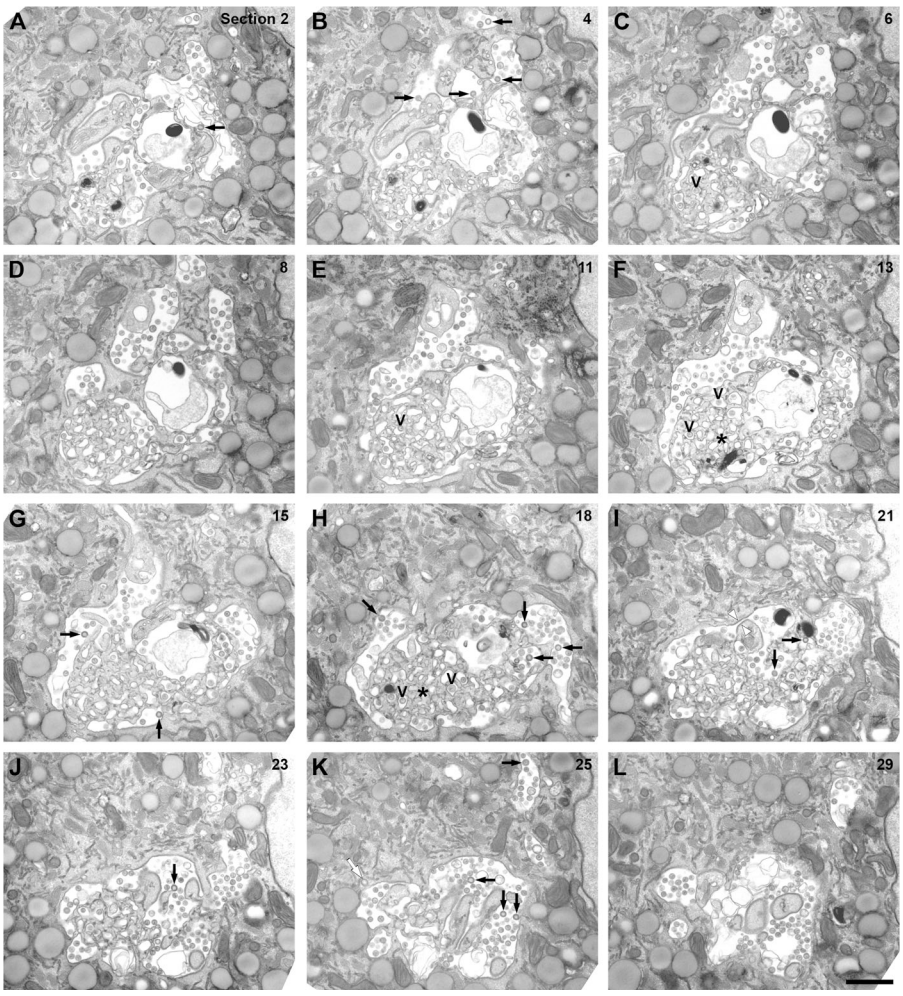

Figure 7. **Serial sections of VCC in HIV-infected MDM.** MDMs infected with HIV for 13 d were fixed, embedded in Epon, and serial ultrathin sections were cut through the virus-containing areas. The images shown were prepared from a series of 29 consecutive 70–80-nm sections (the section number relative to the first section in the set is indicated in the top right corner of each panel). Note the spongelike interconnected membranes, particularly in the more central sections of the set (F and H, asterisks). V marks selected virus particles embedded within the spongelike structures (in C, E, F, and H), white arrowheads indicate coated apposed membranes in I, the white arrow in K marks a coated pit, and the black arrows (in A, B, G–J, and K) identify budding viruses or immature HIV particles. Bar, 1 μm.

HIV infection changes the CD81/CD9/CD53 compartment in MDMs

Although it appears that HIV targets the CD81/CD9/CD53 compartment, there are some differences between the CD81/CD9/CD53-labeled structures observed in uninfected MDMs and the VCCs in HIV-infected macrophages. The CD81/CD9/CD53-labeled structures were usually observed near the bottom of the cell (Fig. 2), whereas the VCCs were often found in higher, more medial confocal sections (Fig. 1). Furthermore, VCCs often appeared enlarged or expanded compared with the CD81/CD9/CD53-labeled structures in uninfected MDMs.

The most striking difference, however, was in the distribution of CD63 relative to the CD81/CD9/CD53 compartment. On uninfected MDMs, there was no overlap between the late endosome marker CD63 and CD81, CD9, or CD53 (Fig. 2 E), whereas infected MDMs showed colabeling of viral p17 and CD63 (Fig. 1 and S1; Raposo et al., 2002; Pelchen-Matthews et al., 2003). This suggests that CD63 must be recruited to the VCCs in HIV-infected MDMs. To investigate whether CD63 trafficking over the cell surface has access to the VCCs, we incubated HIV-infected macrophages with an anti-CD63 mAb for 3 h at 37°C. Cells were then washed, fixed, permeabilized, and

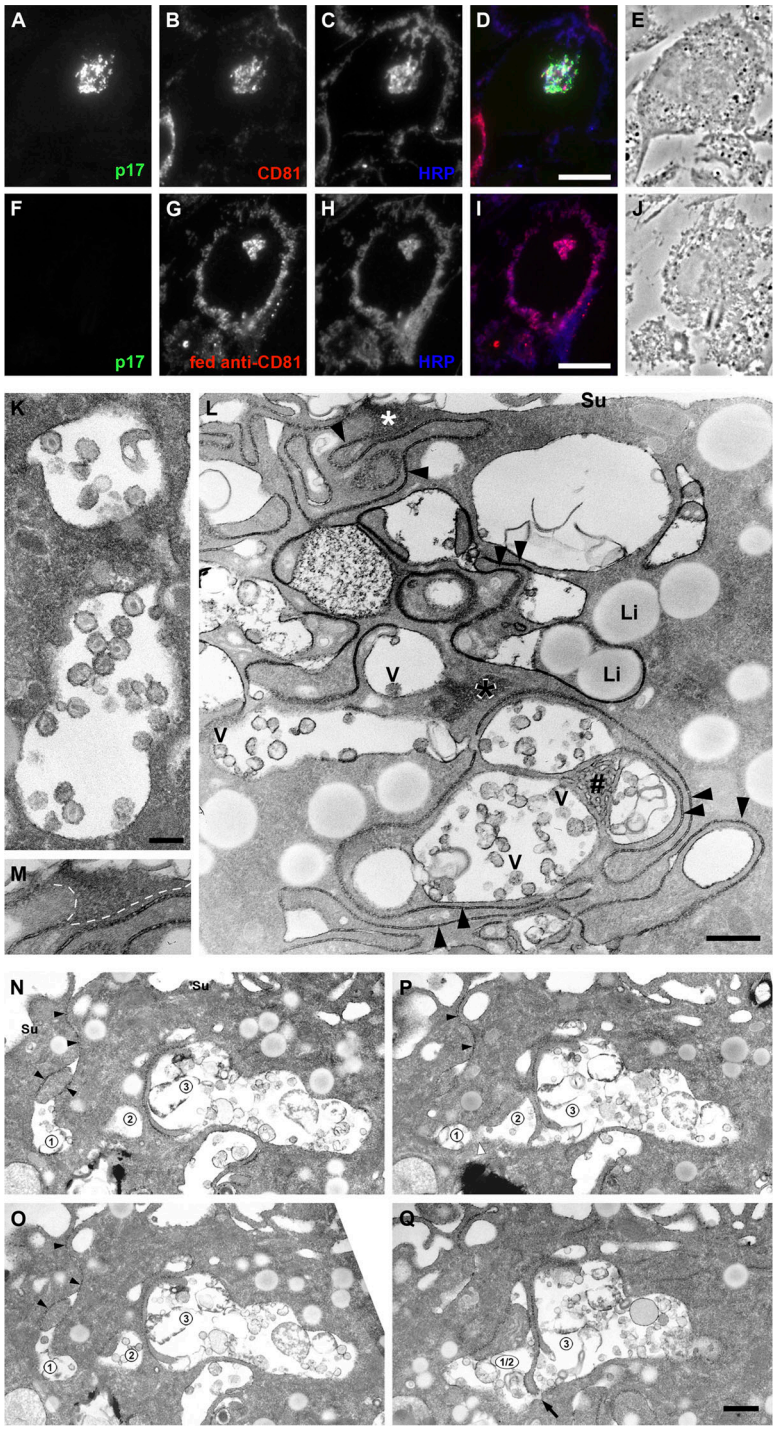

Figure 8. **The intracellular VCCs are accessible from the cell surface.** (A–J) The fluid tracer HRP has access to the VCCs. MDMs infected with HIV for 8 d (A–E) or uninfected MDMs cultured for 13 d and incubated with anti-CD81 for 3 h at 37°C (F-J) were cooled on ice and incubated for 1 h at 4°C with 10 mg/ml HRP. Cells were fixed and processed for cryosectioning. Semithin (0.5 μm thick) sections were triple-stained with anti-p17 mouse IgG2a (A and F, visualized with anti–IgG2a-Alexa Fluor 488, green), anti-CD81 mouse IgG1 (B, anti-IgG1-Alexa Fluor 594, red, or in G, second antibody only) and rabbit anti-HRP (C and H, anti–rabbit-Alexa Fluor 697, blue). Merged immunofluorescence (D and I) and phase-contrast (E and J) images of the sections. HRP reached the CD81-labeled virus-containing structures (D) or the structure containing the fed anti-CD81 (I). (K–Q) MDMs infected with HIV for 13 d were fixed in the presence of RR and embedded in Epon. RR marks surface-accessible membranes with a flocculated, electron-dense deposit. In K, virus particles inside VCCs were coated with RR. L shows extended closely apposed membrane sheets (black arrowheads) near the cell surface (Su) or deep in the cell. The asterisks mark RR-stained membranes cut parallel to the section; the area under the white asterisk links these structures to the cell surface (see the enlargement in M). #, interconnected spongelike membranes deep in the cell. V, virus particles; Li, lipid droplets. (N–Q) Sections 28, 27, 26, and 24, respectively, of a set of 41 serial sections. The black arrowheads in (N and O) mark a thin channel of RR-stained membranes from the cell surface (Su) into VCC 1. In P, VCCs 1 and 2 are coalescing (the edge of the compartment membrane is cut grazingly at the white arrowhead). In Q, VCCs 1 and 2 are fused, and are connected to VCC 3 through a narrow gap (arrow). Bars: (D and I) 10 μm; (K) 200 nm; (L and Q) 500 nm.

stained with antibodies against CD53 and p17. CD53 weakly stained the cell surface, and also labeled several discrete intracellular puncta (Fig. 9 A). In addition, it decorated the VCCs identified by anti-p17 labeling (Fig. 9, B and D). The internalized anti-CD63 mAb was not seen in the tubulovesicular structures that were so prominent in the steady-state staining studies (compare the staining pattern of fed anti-CD63 [Fig. 9] to steady state [Figs. 1 and 2]). Instead, internalized anti-CD63 was seen in dispersed round vesicles and also localized strongly to the VCCs (Fig. 9 C). When we performed anti-CD63 feeding experiments on uninfected MDMs, the internalized anti-CD63 again did not reach the tubulovesicular network within the 3-h time course examined, but was seen in small vesicles dispersed throughout the cytoplasm (Fig. S5 A, available at http://www.jcb.org/cgi/content/full/jcb.200609050/DC1). In a small proportion of these vesicles, the internalized CD63 colocalized with EEA1 (Fig. S5 B) or with CD53 (Fig. S5 C), suggesting that at least a proportion of the cellular CD63 pool cycles over the plasma membrane and passes through early endosomes and the CD81/CD9/CD53 compartment. In HIV-infected cells, this cycling CD63 population may become trapped in the VCCs, perhaps by being incorporated into budding virions (Pelchen-Matthews et al., 2003).

Localization of HIV Env to the CD81/CD9/CD53 compartment in MDMs

The distribution of HIV in infected MDMs has been largely determined using antibodies against the Gag protein. However, the production of infectious particles also requires the viral envelope protein (Env). We studied Env using the human anti-Env mAb 2G12, which binds an epitope covering several N-linked glycosylation sites (Scanlan et al., 2002) and appears to recognize post-ER forms of the viral glycoprotein (Byland et al., 2007). To avoid binding of the mAb to macrophage Fc receptors, $F(ab')_2$ fragments of 2G12 were generated for immunofluorescence staining. Env was observed in the intracellular VCCs, where it colocalized with the capsid protein p24 (Fig. 10 A). Env staining in HIV-infected MDMs also overlapped closely with CD81 (Fig. 10 B). To determine whether Env itself can target the CD81 compartment, Env was expressed in uninfected MDMs by nucleofection. Env was observed almost exclusively in the intracellular CD81-containing compartment (Fig. 10 C) and did not colocalize with the tubulovesicular late endosomes identified by CD63 (Fig. 10 D). As in uninfected MDMs (Fig. 3 A), CD63 and CD81 did not colocalize in the Env-transfected MDMs. Thus, the viral Env glycoprotein appears to be targeted to the CD81/CD9/CD53 compartment.

Discussion

In this study, we have further characterized the compartment where HIV assembles in MDMs. Although in macrophages HIV particles accumulate in structures with the appearance of vacuoles that contain the late endosome marker CD63, our results indicate that these compartments are not endosomes. Instead, we have shown that the virus assembly sites are marked by the tetraspanins CD81, CD9, and CD53. Immunofluorescence staining of uninfected MDMs indicated that CD81, CD9, and CD53 are present at the plasma membrane and in a population of intracellular puncta that are distinct from EEA1-containing early endosomes or the tubulovesicular late endosomes/lysosomes marked by CD63 and LAMP-1. EM analysis revealed a complex morphology for these structures, with multivesicular-like components, closely apposed extended membrane sheets, extensive interconnected spongelike membranes, and lipid deposits, which are structures that are clearly distinct from endocytic organelles. Notably, both CD9 and CD81 were located on the internal membranes of these structures, suggesting that, in MDMs at least, multivesicular organelles are heterogeneous; CD9 and CD81 do not mark endosomes and, in uninfected cells, CD63 does not localize to the multivesicular CD81/CD9/CD53 compartment. In addition, we now report that the CD81/CD9/CD53

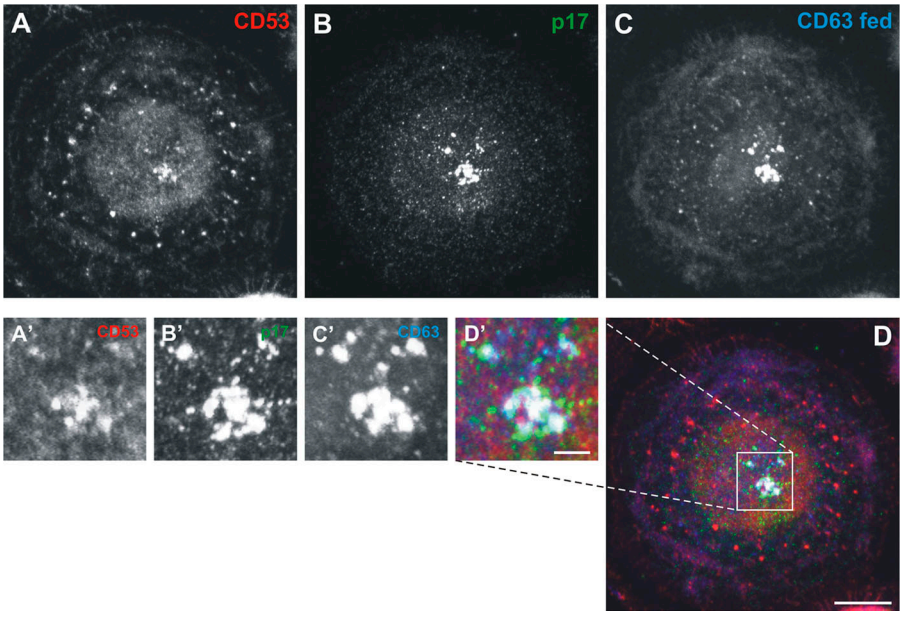

Figure 9. **Anti-CD63 antibodies can access the VCCs.** MDMs infected with HIV for 10 d were incubated for 3 h at 37°C in medium with anti-CD63 (mouse IgG2b). Cells were fixed, permeabilized, and labeled with antibodies against CD53 (mouse IgG1) and p17 (rabbit polyclonal), followed by anti–mouse IgG1-Alexa Fluor 594 and anti–rabbit Alexa Fluor 488. Internalized anti-CD63 was detected with biotin-conjugated anti-IgG2b, followed by Cy5-conjugated streptavidin. (A–C) show the distribution of CD53 (red), viral p17 (green), and internalized anti-CD63 (blue), respectively, whereas D is a merged image. Selected areas are enlarged in (A'–D'). The internalized anti-CD63 accumulated in the VCCs identified by the presence of p17. These VCCs also co-stained for CD53. The images show a projection of 11 confocal sections (0.5 μm thick). Bars: (D) 10 μm; (D') 2.5 μm.

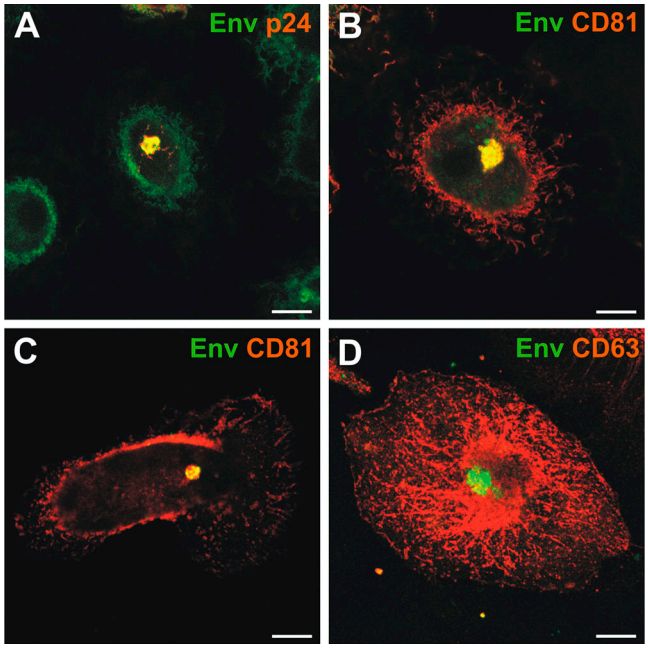

Figure 10. **Immunolocalization of the HIV envelope glycoprotein in MDMs.** (A) MDMs infected with HIV for 10 d were fixed, permeabilized, and stained with mouse mAbs against the HIV capsid protein p24 and $F(ab')_2$ fragments of the human anti-Env mAb 2G12, followed by anti–mouse Alexa Fluor 594 (red) and anti–human FITC (green), respectively. (B) Alternatively, the cells were stained with anti-CD81 and -Env $F(ab')_2$. Env colocalized with assembling virus particles (p24), as well as with CD81. (C and D) Uninfected MDMs were nucleofected with pSVIII HxB2 Env and the distribution of Env was analyzed 48 h after nucleofection, and after treatment with sodium butyrate to boost expression. Fixed and permeabilized cells were double labeled with anti-Env $F(ab')_2$ fragments and antibodies against CD81 (C) or CD63 (D) and secondary antibodies as in A. The images show single confocal sections (0.5 μm thick). Bars, 10 μm.

compartment is linked to the cell surface, both in uninfected and HIV-infected cells, and so may be considered an internally sequestered plasma membrane domain.

In MDMs infected with R5-tropic HIV, mature and immature virus particles and buds were seen in intracellular VCCs, as previously described (Gartner et al., 1986; Gendelman et al., 1988; Orenstein et al., 1988; Sharova et al., 2005; Ryzhova et al., 2006). In observations of a large number of cells on many sections, we saw HIV budding profiles at the limiting membrane of VCCs and on the spongelike membranes and immature virions in the interior (Fig. 6 G and Fig. 7), but not at the cell surface proper. This suggests that the vast majority of HIV particles are formed directly at this site, rather than reaching the intracellular location after endocytosis from the cell surface. Indeed, in infected MDMs, there were very few HIV particles at the cell surface available for endocytosis (Fig. S3 A), and virions were never seen in coated pits or in EEA1-positive early endosomes, as might be expected if virus accessed the VCCs by internalization from the cell surface. The HIV assembly compartment appeared to be derived from a subset of the structures marked by CD81, CD9, and CD53 because (a) immunofluorescence labeling revealed a close overlap of the intracellular virus with these markers, (b) immuno-EM of cryosections showed virus particles associated with structures resembling the CD9- and CD81-containing internal membranes in uninfected MDMs, and (c) an EM analysis of Epon sections of infected MDMs revealed VCCs associated with interconnected spongelike membranes or extended parallel membrane sheets. Although some of the spongelike membranes on Epon sections resemble the paracrystalline ER described in cells overexpressing certain ER proteins (Yamamoto et al., 1996), we did not observe costaining between CD53 or CD81 and the ER marker calnexin (unpublished data).

HIV not only exploits the CD81/CD9/CD53 compartment for assembly, it also changes the compartment. Thus, virus infection expands and/or causes the coalescence of the CD81/CD9/CD53 structures, and it alters their distribution in infected cells. Most significantly, the VCCs also label for CD63, which is in agreement with previous studies (Raposo et al., 2002; Pelchen-Matthews et al., 2003; Ryzhova et al., 2006). However, our present studies indicate that CD63 only reaches the CD81/CD9/CD53 compartment after infection by HIV. Antibody-feeding experiments suggest that a pool of CD63 cycles over the cell surface and through CD81/CD9/CD53-labeled structures and that, in infected MDMs, this cycling CD63 can become trapped in the virus-containing CD81/CD9/CD53 compartment, perhaps through incorporation into HIV particles (Pelchen-Matthews et al., 2003).

Macrophages are unusual in that virus assembly occurs almost exclusively in intracellular VCCs. Nonetheless, experiments in which MDMs were exposed to the fluid tracer HRP at 4°C or fixed in the presence of the membrane-impermeant dye RR indicated that the VCCs are part of an unusual network of surface-connected intracellular structures. As all of the membranes accessed by RR must be connected to the cell surface, they should strictly be classified as plasma membrane. Indeed, the intracellular, CD9-labeled membranes contain the plasma membrane lipid $PI(4,5)P_2$, as demonstrated in preliminary experiments with the phospholipase Cδ1 PH domain linked to GFP (unpublished data). Thus, in MDMs, as in other cells, HIV components appear to be targeted to the $PI(4,5)P_2$-containing plasma membrane, but this domain, though linked to the cell surface, is sequestered within the cell. These observations are consistent with recently published data indicating that HIV assembly does not occur on endosomes, but that the viral Gag protein is directly targeted to the plasma membrane (Jouvenet et al., 2006; Neil et al., 2006). To date, we have only seen the CD9- or CD81-labeled intracellular structures in MDMs or in some LPS-matured monocyte-derived DCs, but the compartment is rare and difficult to find, even in these cells. Thus, we cannot be sure whether similar structures exist in other cells, such as T cells or HeLa, which express the tetraspanins CD9 and CD81 at lower levels. The surface-connected structures in macrophages may be related to the surface-connected patocytosis compartment that is involved in the uptake and sequestration of aggregated cholesterol (Kruth, 2002).

How the viral components are targeted to the intracellular CD81/CD9/CD53-containing membranes is unclear. Virus assembly may be stabilized at this compartment by the tetraspanins, as it has been suggested that HIV assembly may be gated

through tetraspanin-enriched microdomains (Nydegger et al., 2006). It seems unlikely, however, that virus targeting to tetraspanin domains alone accounts for targeting to the VCCs because high levels of CD9 or CD81 are also found at the cell surface in MDMs, whereas the bulk of CD63 is in distinct late endosomes/lysosomes. Indeed, even within the CD81/CD9/CD53 compartment, most of the tetraspanins appear to be sequestered on the internal membranes. When the HIV Env protein was expressed alone in MDMs after transfection, it localized to intracellular vesicles that costained with CD81, but did not relocate CD63 to these structures, suggesting that other viral proteins are required for CD63 accumulation in the virus assembly compartment.

Assembly in the CD81/CD9/CD53 compartment appears to offer several advantages for HIV. The compartment contains large amounts of membrane that can be used by the virus to form its envelopes. The assembled virus particles may then be stored in an infectious form until they are released (Sharova et al., 2005). By EM, the channels that connect the virus-containing structures to the cell surface are very narrow (<20 nm on Epon sections), suggesting that although RR (Mr = 786) or HRP (40 kD) can pass through these gaps, the diffusion of larger antibody molecules, which are ~10 nm long, may be impeded, and virus particles with diameters of 120–140 nm are retained in the cells. Generally, the spacing between the membrane sheets appeared very regular, even over extended distances (Fig. 8 L and Fig. S3), suggesting that proteins lining the membrane—perhaps together with the tetraspanins—support these structures. In some regions, we observed flat coats and cytoskeletal meshworks, presumably actin, associated with the membrane tracks; these structures may further support membranes in the closely apposed configuration and perhaps regulate access. Indeed, treatment with cytochalasin D has been reported to disrupt the VCCs in MDMs (Jouvenet et al., 2006). Because the VCCs are connected to the cell surface, virions would be in contact with the extracellular, most likely neutral, pH and not the harsh acidic/degradative environment of endosomes, and any stimuli that would open the connecting membrane channels would lead to the rapid release of virus particles, together with CD81/CD9-containing exosomes and other membrane structures present in the VCCs.

The possibility that HIV may be released from the CD81/CD9/CD53 structures in a regulated manner is also suggested by analogy to the interaction of HIV with DCs, where compartments marked by CD81 may play a role during antigen presentation. CD81 has been shown to redistribute to the immunological synapse between T cells and either B cells or DCs, in an antigen-dependent manner (Mittelbrunn et al., 2002). DCs, at least in tissue culture, are able to capture extracellular virus particles and later release them onto T cells for infection in trans (Kwon et al., 2002; McDonald et al., 2003; Garcia et al., 2005). The compartments into which HIV is internalized in DCs resemble the VCCs of MDMs in their size and complexity, internal vesicles and membranes that label for CD81 or CD9, clathrin-coated pits, and extended areas of thickened flat coats. Notably, the DC virus-containing structures also lack markers for early endosomes or late endosomes and lysosomes and stain only weakly for CD63 (Garcia et al., 2005). In DCs, HIV can access the compartment by uptake from the cell surface, whereas in MDMs, virus assembles directly into the CD81/CD9/CD53 compartment. The similarities between the viral compartments of DCs and MDMs suggest that the macrophage compartment may also be involved in virus transfer to target cells. Such processes are likely to involve complex membrane rearrangements. In this respect, the narrow membrane channels and surface connections from the MDM VCCs show some resemblance to the tubules induced during stimulation of murine DCs (Boes et al., 2002; Chow et al., 2002).

MDMs are primary cells, but, as they have undergone differentiation in culture, we cannot be sure that the structures we describe in this study are present in macrophages in vivo, though intracellular assembly of virus was observed with both HIV types 1 and 2 and in brain macrophages of an individual with AIDS encephalopathy (Orenstein et al., 1988). Macrophages are widely distributed in all tissues and organs and are believed to be an important vehicle for spreading HIV infection to $CD4^+$ T cells (Herbein et al., 2002), perhaps because they sequester virus in intracellular compartments. Indeed, the HIV sequestered in MDMs can remain infectious for many days (Sharova et al., 2005). By analogy with studies on DCs, macrophages may likewise release HIV from the CD81/CD9/CD53-containing VCCs when they encounter T cells (Sharova et al., 2005). For HIV, virological synapses have been described for conjugates between DCs and T cells or between infected and uninfected T cells (Piguet and Sattentau, 2004), and macrophages have been shown to release HIV particles onto epithelial cells (Bourinbaiar and Phillips, 1991) or peripheral blood lymphocytes (Carr et al., 1999) in a directed manner. The CD81/CD9/CD53 compartment may function in the formation or activity of immunological synapses, and it is these properties that are exploited by HIV to facilitate cell–cell transfer through virological synapses. Moreover, the potential to hide virus intracellularly, beyond the reach of humoral immune responses, may have important implications for vaccine design and AIDS pathogenesis.

Materials and methods

Reagents and antibodies

Tissue culture media and supplements were obtained from Invitrogen, and tissue culture plastic was purchased from TPP. HRP type II and other chemicals were obtained from Sigma-Aldrich, unless stated otherwise.

The mouse mAb against CD63 (1B5 and IgG2b) has been previously described (Fraile-Ramos et al., 2001); anti-CD81 (M38, IgG1) was provided by F. Berditchevski (University of Birmingham, Birmingham, UK); anti-CD53 (MEM-53 and IgG1) and anti-CD9 (MCA469GA and IgG2b) were purchased from Abcam and Serotec, respectively; anti–LAMP-1 (H4A3 and IgG1) and anti-EEA1 (clone 14 and IgG1) were obtained from BD Biosciences. mAbs to HIV p17 (4C9, mouse IgG2a, and ARP342 were obtained from R.B. Ferns and R.S. Tedder, Middlesex Hospital Medical School, London UK), p24 (mAbs 38:96K and EF7, both mouse IgG1, ARP365, and 366, respectively, from B. Wahren, National Bacteriological Laboratory, Stockholm, Sweden), and Env (human mAb 2G12, EVA3064; obtained from H. Katinger, Institute of Applied Microbiology, Vienna, Austria) were obtained through the National Institute for Biological Standards and Control Centralised Facility for AIDS Reagents, which is supported by the EU Program EVA and the UK Medical Research Council. $F(ab')_2$ fragments of 2G12 were generated using the ImmunoPure Preparation kit (Pierce). The rabbit antiserum UP595 against HIV p17 was provided by

M. Malim (Guy's, King's and St Thomas' School of Medicine, London, UK), rabbit anti-HRP was purchased from Jackson ImmunoResearch Laboratories, rabbit anti–mouse bridging antibody was purchased from DakoCytomation, and biotin-conjugated anti-IgG2b was purchased from Southern Biotechnology Associates. Alexa Fluor–labeled fluorescent antibodies were obtained from Invitrogen, Cy5-streptavidin was purchased from Jackson ImmunoResearch Laboratories, and FITC goat anti–human was obtained from Pierce Chemical Co. PAG reagents were obtained from the EM Lab (Utrecht University, Utrecht, Netherlands).

Cells and viruses

Peripheral blood mononuclear cells (PBMCs) were prepared from buffy coats from healthy donors (National Blood Service, Essex, UK), and adherent monocytes were isolated as previously described (Pelchen-Matthews et al., 2003). Monocytes were differentiated to MDMs in complete medium (RPMI 1640, 100 U/ml penicillin, 0.1 mg/ml streptomycin, and 10% human AB serum [PAA Laboratories] with 10 ng/ml of M-CSF [R&D Systems]) for 2 d, and then differentiated without M-CSF until required.

HIV-1_{BaL} was obtained from R. Shattock (St. George's Hospital, London, UK). A first virus stock was prepared by infection of PHA-stimulated PBMC (grown in RPMI 1640 with penicillin, streptomycin, 10% FCS, and 20 U/ml Il-2 [R&D Systems] and treated for 3 d with 0.5 μg/ml PHA-P). PBMC-grown HIV-1_{BaL} was passaged once through MDMs to maintain tropism. Cell-free supernatants were harvested every 3 d, aliquoted, and stored in liquid nitrogen. Virus titers were determined on NP2-CD4-CCR5 cells as previously described (Pelchen-Matthews et al., 2003).

For experiments, MDMs were infected 6 d after isolation with HIV-1_{BaL} (2 FFU/cell) by spinoculation at 2.5 krpm for 2 h at RT, and cultured for various times as indicated. For infectivity assays, NP2-CD4-CCR5, were inoculated by spinoculation as above, and stained with X-Gal after 3 d (Pelchen-Matthews et al., 2003).

Nucleofection of HIV Env protein

MDMs were grown for 7 d, detached using trypsin/EDTA, and nucleofected with pSVIII HxB2 Env (Helseth et al., 1990), using a Nucleofector with the macrophage nucleofection kit and program Y-10 (Amaxa).

Immunofluorescence staining of whole-cell preparations

MDMs were fixed by adding an equal volume of double-strength fixative, 6% PFA (TAAB Laboratories) to the culture medium for ~30 min at RT. After washing, free-aldehyde groups were quenched with 50 mM NH_4Cl, and the cells were permeabilized for 1 h in blocking buffer (0.1% saponin and 0.5% BSA in PBS) containing 10 μg/ml purified human IgG. Cells were stained with primary antibodies diluted in blocking buffer for 1 h, washed, and incubated for 1 h with appropriate combinations of fluorescent secondary antibodies. Coverslips were mounted in Mowiol (Merck), and examined directly or stored at –20°C. Staining was analyzed with a microscope (Optiphot-2; Nikon) equipped with an upright confocal laser scanner and a Plan Apochromat 60× oil-immersion lens (Nikon) and an upright confocal laser scanner (MRC 1024; Bio-Rad Laboratories). Images were acquired at RT using LaserSharp2000 (Bio-Rad Laboratories) and processed using Photoshop (Adobe) or ImageJ (National Institutes of Health). Volocity version 3.6.1 was used to measure colocalization.

For some experiments, HIV-infected or uninfected MDMs were incubated for 3 h at 37°C (or as a control at 4°C) with antibodies against CD9 (4 μg/ml), CD81 (13.5 μg/ml), CD63 (1 μg/ml), or CD53 (20 μg/ml) in complete medium, washed, and processed for immunofluorescence as in the previous paragraph.

EM methods

HIV-infected MDMs were fixed for 4 h in 2% PFA/3% glutaraldehyde in 0.1 M NaPi buffer, pH 7.4, postfixed for 1 h on ice in 1% OsO_4/1.5% $K_3[Fe(CN)_6]$, and treated with 1.5% tannic acid (Simionescu and Simionescu, 1976). To test accessibility to the cell surface, some samples were fixed for 4 h in the fixative containing 5 mg/ml RR, postfixed 2 h in 1% OsO_4/5 mg/ml RR, and stained for 1 h in 1% uranyl acetate. Samples were dehydrated in graded ethanols and embedded in Epon 812 (TAAB Laboratories). Ultrathin sections were cut on an Ultracut UCT ultramicrotome (Leica) and stained with lead citrate (sections of RR-treated cells remained unstained).

For immunolabeling, HIV-infected MDMs or uninfected control cells were fixed by adding an equal volume of prewarmed double-strength fixative (8% PFA in 0.1 M NaPi buffer, pH7.4) directly into the culture medium. After 10 min, the medium was replaced with 4% PFA. Cells were rinsed in PBS containing 20 mM glycine, embedded in 12% gelatine, infiltrated with 2.3 M sucrose, and frozen in liquid nitrogen as previously described (Raposo et al., 1997). Semithin (0.5 μm) or ultrathin (50 nm) cryosections were cut on an Ultracut UCT microtome equipped with an EM FCS cryochamber.

Immunofluorescence staining. Semithin cryosections on glass slides were quenched in 50 mM glycine/50 mM NH_4Cl, labeled with antibodies diluted in PBS 1% BSA, and mounted in Mowiol. Sections were examined at RT with a microscope (Axioskop; Carl Zeiss MicroImaging, Inc.) fitted with Plan Neofluar oil immersion objectives (63×/1.25 NA or 100×/1.30 NA). Images were recorded with a charge-coupled device camera (Orca C4742-95; Hamamatsu) controlled by Openlab 3.1.7 software (Improvision), false colored, converted to TIFF files, adjusted for brightness and contrast and assembled into montages with Photoshop 8.

EM immunolabeling. Ultrathin cryosections on formvar-coated grids were quenched as above and labeled with primary antibodies and PAG (5, 10, or 15 nm). Sections stained with mouse mAb were incubated with a rabbit anti–mouse bridging antibody before labeling with PAG. For double labeling, cells were first stained with mouse mAbs, the rabbit anti–mouse bridging antibody, and PAG, and fixed in 1% glutaraldehyde for 10 min before requenching and staining with a rabbit antiserum against HIV p17. Sections were examined with an EM420 (Philips) or a CM10 transmission EM (FEI), and images were recorded onto electron image film (SO-163; Kodak). Negatives were digitized with a FlexTight Precision II rotating drum charge-coupled device scanner (Imacon), and TIFF images were acquired with the ColorFlex 1.9.5 FlexTight Interface Software. Alternatively, specimens were examined with a Tecnai G2 Spirit transmission EM (FEI) and digital images were recorded with a Morada 11 MegaPixel TEM camera (Soft Imaging System) and the AnalySIS software package. Images were adjusted for brightness and contrast and figures were assembled with Photoshop 8.

Online supplemental material

Fig. S1 shows immunofluorescence staining for HIV and CD63, CD81, or CD9 on semithin cryosections. Fig. S2 shows control experiments for the feeding of anti-CD81 or -CD9. Fig. S3 shows how closely apposed membrane sheets connect different VCCs, and Fig. S4 shows serial sections of VCCs in HIV-infected MDMs. Fig. S5 shows feeding of anti-CD63 on uninfected MDMs. The online version of this article is available at http://www.jcb.org/cgi/content/full/jcb.200609050/DC1.

We thank Aine McKnight and Robin Weiss for access to the P3 containment laboratory, Lucy Collinson for serial sectioning, and Graça Raposo, Vincent Piguet, Lars Hinrichsen, and Tom Kershaw for helpful comments on the manuscript. We are grateful to the National Institute for Biological Standards and Control Centralised Facility for AIDS Reagents and to Fedor Berditchevski and Michael Malim for providing antibody reagents.

M. Deneka was supported by a European Molecular Biology Organization long-term fellowship ALTF 956-2003, E. Ruiz-Mateos was supported by Fondo de Investigacion Sanitaria grant CD05/00174, and R. Byland by National Institutes of Health grant AI-49784 to James A. Hoxie and M. Marsh. A. Pelchen-Matthews and M. Marsh were supported by UK Medical Research Council funding to the Cell Biology Unit.

Submitted: 8 September 2006
Accepted: 20 March 2007

Note added in proof. During preparation of this manuscript for publication, similar observations were reported by Welsh et al. (Welsch, S., O.T. Keppler, A. Habermann, I. Allespach, J. Krijnse-Locker, and H.G. Krausslich. 2007. *PLoS Pathog.* 3:e36.).

References

Astarie-Dequeker, C., S. Carreno, C. Cougoule, and I. Maridonneau-Parini. 2002. The protein tyrosine kinase Hck is located on lysosomal vesicles that are physically and functionally distinct from CD63-positive lysosomes in human macrophages. *J. Cell Sci.* 115:81–89.

Boes, M., J. Cerny, R. Massol, M. Op den Brouw, T. Kirchhausen, J. Chen, and H.L. Ploegh. 2002. T-cell engagement of dendritic cells rapidly rearranges MHC class II transport. *Nature*. 418:983–988.

Booth, A.M., Y. Fang, J.K. Fallon, J.M. Yang, J.E.K. Hildreth, and S.J. Gould. 2006. Exosomes and HIV Gag bud from endosome-like domains of the T cell plasma membrane. *J. Cell Biol.* 172:923–935.

Bourinbaiar, A.S., and D.M. Phillips. 1991. Transmission of human immunodeficiency virus from monocytes to epithelia. *J. Acquir. Immune Defic. Syndr.* 4:56–63.

Byland, R., P.J. Vance, J.A. Hoxie, and M. Marsh. 2007. A conserved dileucine motif mediates clathrin and AP-2-dependent endocytosis of the HIV-1 envelope protein. *Mol. Biol. Cell*. 18:414–425.

Carr, J.M., H. Hocking, P. Li, and C.J. Burrell. 1999. Rapid and efficient cell-to-cell transmission of human immunodeficiency virus infection from monocyte-derived macrophages to peripheral blood lymphocytes. *Virology*. 265:319–329.

Chow, A., D. Toomre, W. Garrett, and I. Mellman. 2002. Dendritic cell maturation triggers retrograde MHC class II transport from lysosomes to the plasma membrane. *Nature*. 418:988–994.

Escola, J.M., M.J. Kleijmeer, W. Stoorvogel, J.M. Griffith, O. Yoshie, and H.J. Geuze. 1998. Selective enrichment of tetraspan proteins on the internal vesicles of multivesicular endosomes and on exosomes secreted by human B-lymphocytes. *J. Biol. Chem.* 273:20121–20127.

Fraile-Ramos, A., T.N. Kledal, A. Pelchen-Matthews, K. Bowers, T.W. Schwartz, and M. Marsh. 2001. The human cytomegalovirus US28 protein is located in endocytic vesicles and undergoes constitutive endocytosis and recycling. *Mol. Biol. Cell*. 12:1737–1749.

Fritzsching, B., B. Schwer, J. Kartenbeck, A. Pedal, V. Horejsi, and M. Ott. 2002. Release and intercellular transfer of cell surface CD81 via microparticles. *J. Immunol.* 169:5531–5537.

Garcia, E., M. Pion, A. Pelchen-Matthews, L. Collinson, J.F. Arrighi, G. Blot, F. Leuba, J.M. Escola, N. Demaurex, M. Marsh, and V. Piguet. 2005. HIV-1 trafficking to the dendritic cell-T-cell infectious synapse uses a pathway of tetraspanin sorting to the immunological synapse. *Traffic*. 6:488–501.

Gartner, S., P. Markovits, D.M. Markovitz, M.H. Kaplan, R.C. Gallo, and M. Popovic. 1986. The role of mononuclear phagocytes in HTLV-III/LAV infection. *Science*. 233:215–219.

Gendelman, H.E., J.M. Orenstein, M.A. Martin, C. Ferrua, R. Mitra, T. Phipps, L.A. Wahl, H.C. Lane, A.S. Fauci, and D.S. Burke,. 1988. Efficient isolation and propagation of human immunodeficiency virus on recombinant colony-stimulating factor 1-treated monocytes. *J. Exp. Med.* 167:1428–1441.

Grigorov, B., F. Arcanger, P. Roingeard, J.L. Darlix, and D. Muriaux. 2006. Assembly of infectious HIV-1 in human epithelial and T-lymphoblastic cell lines. *J. Mol. Biol.* 359:848–862.

Harila, K., I. Prior, M. Sjoberg, A. Salminen, J. Hinkula, and M. Suomalainen. 2006. Vpu and Tsg101 regulate intracellular targeting of the human immunodeficiency virus type 1 core protein precursor Pr55gag. *J. Virol.* 80:3765–3772.

Helseth, E., M. Kowalski, D. Gabuzda, U. Olshevsky, W. Haseltine, and J. Sodroski. 1990. Rapid complementation assays measuring replicative potential of human immunodeficiency virus type 1 envelope glycoprotein mutants. *J. Virol.* 64:2416–2420.

Herbein, G., A. Coaquette, D. Perez-Bercoff, and G. Pancino. 2002. Macrophage activation and HIV infection: can the Trojan horse turn into a fortress? *Curr. Mol. Med.* 2:723–738.

Heuser, J. 1989. Changes in lysosome shape and distribution correlated with changes in cytoplasmic pH. *J. Cell Biol.* 108:855–864.

Jouvenet, N., S.J. Neil, C. Bess, M.C. Johnson, C.A. Virgen, S.M. Simon, and P.D. Bieniasz. 2006. Plasma membrane is the site of productive HIV-1 particle assembly. *PLoS Biol.* 4:e435.

Kobayashi, T., U.M. Vischer, C. Rosnoblet, C. Lebrand, M. Lindsay, R.G. Parton, E.K. Kruithof, and J. Gruenberg. 2000. The tetraspanin CD63/lamp3 cycles between endocytic and secretory compartments in human endothelial cells. *Mol. Biol. Cell*. 11:1829–1843.

Kramer, B., A. Pelchen-Matthews, M. Deneka, E. Garcia, V. Piguet, and M. Marsh. 2005. HIV interaction with endosomes in macrophages and dendritic cells. *Blood Cells Mol. Dis.* 35:136–142.

Kruth, H.S. 2002. Sequestration of aggregated low-density lipoproteins by macrophages. *Curr. Opin. Lipidol.* 13:483–488.

Kwon, D.S., G. Gregorio, N. Bitton, W.A. Hendrickson, and D.R. Littman. 2002. DC-SIGN-mediated internalization of HIV is required for trans-enhancement of T cell infection. *Immunity*. 16:135–144.

McDonald, D., L. Wu, S.M. Bohks, V.N. KewalRamani, D. Unutmaz, and T.J. Hope. 2003. Recruitment of HIV and its receptors to dendritic cell-T cell junctions. *Science*. 300:1295–1297.

Mittelbrunn, M., M. Yanez-Mo, D. Sancho, A. Ursa, and F. Sanchez-Madrid. 2002. Cutting edge: dynamic redistribution of tetraspanin CD81 at the central zone of the immune synapse in both T lymphocytes and APC. *J. Immunol.* 169:6691–6695.

Neil, S.J., S.W. Eastman, N. Jouvenet, and P.D. Bieniasz. 2006. HIV-1 Vpu promotes release and prevents endocytosis of nascent retrovirus particles from the plasma membrane. *PLoS Pathog.* 2:e39.

Nguyen, D.G., A. Booth, S.J. Gould, and J.E. Hildreth. 2003. Evidence that HIV budding in primary macrophages occurs through the exosome release pathway. *J. Biol. Chem.* 278:52347–52354.

Nydegger, S., M. Foti, A. Derdowski, P. Spearman, and M. Thali. 2003. HIV-1 egress is gated through late endosomal membranes. *Traffic*. 4:902–910.

Nydegger, S., S. Khurana, D.N. Krementsov, M. Foti, and M. Thali. 2006. Mapping of tetraspanin-enriched microdomains that can function as gateways for HIV-1. *J. Cell Biol.* 173:795–807.

Ono, A., S.D. Ablan, S.J. Lockett, K. Nagashima, and E.O. Freed. 2004. Phosphatidylinositol (4,5) bisphosphate regulates HIV-1 Gag targeting to the plasma membrane. *Proc. Natl. Acad. Sci. USA*. 101:14889–14894.

Orenstein, J.M., M.S. Meltzer, T. Phipps, and H.E. Gendelman. 1988. Cytoplasmic assembly and accumulation of human immunodeficiency virus types 1 and 2 in recombinant human colony-stimulating factor-1-treated human monocytes: an ultrastructural study. *J. Virol.* 62:2578–2586.

Pelchen-Matthews, A., B. Kramer, and M. Marsh. 2003. Infectious HIV-1 assembles in late endosomes in primary macrophages. *J. Cell Biol.* 162:443–455.

Perlman, M., and M.D. Resh. 2006. Identification of an intracellular trafficking and assembly pathway for HIV-1 Gag. *Traffic*. 7:731–745.

Piguet, V., and Q. Sattentau. 2004. Dangerous liaisons at the virological synapse. *J. Clin. Invest.* 114:605–610.

Raposo, G., M.J. Kleijmeer, G. Posthuma, J.W. Slot, and H.J. Geuze. 1997. Immunogold labeling of ultrathin cryosections: application in immunology. *In* Handbook of Experimental Immunology. L.A. Herzenberg, D.M. Weir, L.A. Herzenberg, and C. Blackwell editors. Blackwell Science, Inc. Oxford, UK. pp. 1–11.

Raposo, G., M. Moore, D. Innes, R. Leijendekker, A. Leigh-Brown, P. Benaroch, and H. Geuze. 2002. Human macrophages accumulate HIV-1 particles in MHC II compartments. *Traffic*. 3:718–729.

Resh, M.D. 2005. Intracellular trafficking of HIV-1 Gag: how Gag interacts with cell membranes and makes viral particles. *AIDS Rev.* 7:84–91.

Robinson, J.M., J. Chiplonkar, and Z. Luo. 1996. A method for co-localization of tubular lysosomes and microtubules in macrophages: fluorescence microscopy of individual cells. *J. Histochem. Cytochem.* 44:1109–1114.

Ryzhova, E.V., R.M. Vos, A.V. Albright, A.V. Harrist, T. Harvey, and F. Gonzalez-Scarano. 2006. Annexin 2: a novel human immunodeficiency virus type 1 Gag binding protein involved in replication in monocyte-derived macrophages. *J. Virol.* 80:2694–2704.

Saad, J.S., J. Miller, J. Tai, A. Kim, R.H. Ghanam, and M.F. Summers. 2006. Structural basis for targeting HIV-1 Gag proteins to the plasma membrane for virus assembly. *Proc. Natl. Acad. Sci. USA*. 103:11364–11369.

Scanlan, C.N., R. Pantophlet, M.R. Wormald, E. Ollmann Saphire, R. Stanfield, I.A. Wilson, H. Katinger, R.A. Dwek, P.M. Rudd, and D.R. Burton. 2002. The broadly neutralizing anti-human immunodeficiency virus type 1 antibody 2G12 recognizes a cluster of alpha1→2 mannose residues on the outer face of gp120. *J. Virol.* 76:7306–7321.

Sharova, N., C. Swingler, M. Sharkey, and M. Stevenson. 2005. Macrophages archive HIV-1 virions for dissemination in trans. *EMBO J.* 24:2481–2489.

Sherer, N.M., M.J. Lehmann, L.F. Jimenez-Soto, A. Ingmundson, S.M. Horner, G. Cicchetti, P.G. Allen, M. Pypaert, J.M. Cunningham, and W. Mothes. 2003. Visualization of retroviral replication in living cells reveals budding into multivesicular bodies. *Traffic*. 4:785–801.

Simionescu, N., and M. Simionescu. 1976. Galloylglucoses of low molecular weight as mordant in electron microscopy. I. Procedure, and evidence for mordanting effect. *J. Cell Biol.* 70:608–621.

Swanson, J., A. Bushnell, and S.C. Silverstein. 1987. Tubular lysosome morphology and distribution within macrophages depend on the integrity of cytoplasmic microtubules. *Proc. Natl. Acad. Sci. USA*. 84:1921–1925.

Thery, C., A. Regnault, J. Garin, J. Wolfers, L. Zitvogel, P. Ricciardi-Castagnoli, G. Raposo, and S. Amigorena. 1999. Molecular characterization of dendritic cell-derived exosomes: selective accumulation of the heat shock protein hsc73. *J. Cell Biol.* 147:599–610.

Yamamoto, A., R. Masaki, and Y. Tashiro. 1996. Formation of crystalloid endoplasmic reticulum in COS cells upon overexpression of microsomal aldehyde dehydrogenase by cDNA transfection. *J. Cell Sci.* 109(Pt 7):1727–1738.